PROTEINS: Structure, Function, and Genetics 32:229–240 (1998)

Role of Water in Plasticity, Stability, and Action of Proteins: The Crystal Structures of Lysozyme at Very Low Levels of Hydration

H.G. Nagendra, N. Sukumar, and M. Vijayan*
Molecular Biophysics Unit, Indian Institute of Science, Bangalore, India

ABSTRACT **Earlier studies involving water-mediated transformations in lysozyme and ribonuclease A have shown that the overall movements in the protein molecule consequent to the reduction in the amount of surrounding water are similar to those that occur during enzyme action, thus highlighting the relationship among hydration, plasticity, and action of these enzymes. Monoclinic lysozyme retains its crystallinity even when the level of hydration is reduced further below that necessary for activity (about 0.2 gram of water per gram of protein). In order to gain insights into the role of water in the stability and the plasticity of the protein molecule and the geometrical basis for the loss of activity that accompanies dehydration, the crystal structures of monoclinic lysozyme with solvent contents of 17.6%, 16.9%, and 9.4% were determined and refined. A detailed comparison of these forms with the normally hydrated forms show that the C-terminal segment (residues 88–129) of domain I and the main loop (residues 65–73) in domain II exhibit large deviations in atomic positions when the solvent content is reduced, although the three-dimensional structure is essentially preserved. Many crucial water bridges between different regions of the molecule are conserved in spite of differences in detail, even when the level of hydration is reduced well below that required for activity. The loss of activity that accompany dehydration appears to be caused by the removal of functionally important water molecules from the active-site region and the reduction in the size of the substrate binding cleft. Proteins 32:229–240, 1998.** © 1998 Wiley-Liss, Inc.

Key words: active-site geometry; crystal structure; enzyme action; protein hydration; protein mobility

INTRODUCTION

The importance of water in biological systems can hardly be overemphasized. The major component of all living organisms is water. The folding, structure, mobility, function, and properties of biomolecules such as proteins and nucleic acids and biological multimolecular assemblies such as membranes all depend on the aqueous environment. Therefore, understandably, biomolecular hydration and its consequences have been studied extensively.[1–13]

Protein–water interactions and their consequences have received particular attention. A wealth of detailed information on such interactions has emerged during the last couple of decades from high-resolution protein crystallographic studies.[14–23] More recently, NMR studies have also begun to yield information on protein–water interactions.[24–26] These studies have led to a general picture in which each protein molecule is surrounded by a hydration shell consisting of ordered water molecules directly attached to protein atoms. The water molecules become rapidly disordered as their distance from the protein surface increases and fade into bulk water. Careful examination of the water structure surrounding protein molecules seems to indicate that each protein molecule is endowed with a characteristic hydration shell that is substantially conserved with respect to environmental effects and even to some extent to species variation.[19] The mobility of protein molecules, which is often related to hydration, has also received considerable attention.[18,19,27–32]

We have been exploring the hydration and the related mobility of proteins using an approach involving water-mediated transformations, in which protein crystals undergo abrupt changes with loss of water when the relative humidity (RH) of the environment is systematically reduced.[33,34] These studies have led to the delineation of the relatively rigid and the flexible regions of the lysozyme and the ribonuclease A molecules, as well as the identification of the invariant features in their hydration shell.[18,19,22] Furthermore, it was demonstrated that the gentle reduction in the quantity of the surrounding water affects the hydration shell of proteins, which in turn leads to perturbations in the protein structure. These perturbations are most pronounced in the regions

Grant sponsor: Department of Science and Technology, Government of India.
*Correspondence to: M. Vijayan, Molecular Biophysics Unit, Indian Institute of Science, Bangalore-560 012, India. E-mail: mv@mbu.iisc.ernet.in
Received 25 November 1997; Accepted 17 February 1998

that move during protein action. In fact, it turns out that the overall changes in the structures of lysozyme and ribonuclease A resulting from partial dehydration are similar to those that occur during substrate binding.[18,22,32] Therefore, it has been possible to establish a relationship among hydration, mobility, and enzyme action using the approach involving water-mediated transformation.

The most spectacular water-mediated transformation observed so far is that in monoclinic lysozyme. The solvent content of the crystals comes down to 22%, in the form obtained at an RH of 88%.[21,34] During the transformation, the two crystallographically independent molecules in the native form become equivalent in the low-humidity form. A detailed analysis of the low-humidity structure and its comparison with the native structure did indeed provide valuable information on the hydration and the mobility of the protein, particularly in relation to its activity.[32] The water content in the low humidity monoclinic lysozyme (22%) was the lowest observed in any protein crystal till then. It turns out that monoclinic lysozyme retains its crystallinity even when the solvent content is reduced still further.[35] We report here the crystal structures of two forms with a solvent content of approximately 17% and another with a solvent content of about 9%.

It has been demonstrated that about 0.2 gram of water per gram of protein is the level of hydration necessary for lysozyme to be active.[4,8] Therefore, considering the approximations involved in estimating the solvent contents,[36] the 17% forms might correspond to a marginal case in terms of activity, whereas the molecules in the form with 9% solvent content is certain to be inactive. Thus, the analysis of these very poorly hydrated forms is likely to provide information as to how the reduction in hydration level impairs activity even when the enzyme retains its three-dimensional structure as evidenced by their crystallinity. Furthermore, the availability of monoclinic forms with different solvent contents would permit a study of the structure of the enzyme molecule at different levels of hydration, particularly in relation to water bridges, which constitute an important component of tertiary interactions. The analysis of different forms would also contribute to the hydration-related plasticity of the enzyme molecule. The 9% solvent content form, which was obtained with concentrated sulfuric acid as the dehydrating agent, perhaps defines the level of hydration essential for maintaining the integrity of the protein molecule.

MATERIALS AND METHODS

Preparation of Crystals and Data Collection

The crystals used in the investigations were grown by the well-known method described in the literature.[37] The two forms with solvent contents of 16.9% and 17.6% were obtained by maintaining the RH in the capillary by placing a few drops of concentrated $Zn(NO_3)_2$ solution[38,39] at a distance of 1 cm from the crystal. A few drops of concentrated sulfuric acid was used instead for maintaining the crystals at an RH of 5%.[39] The forms obtained at 38% RH would be hereafter referred to as W17I and W17II, respectively, and that obtained at 5% RH as W9, in accordance to their solvent contents. Likewise, the two independent molecules in the native crystals[32] (32.3% solvent content) are designated as W32A and W32B, while the 88% RH form[21] with 22% solvent content as W22.

TABLE I. Summary of Data and Refinement Statistics[a]

	W17I	W17II	W9
Space group	$P2_1$	$P2_1$	$P2_1$
a (Å)	26.6	26.3	25.3
b (Å)	56.0	55.9	54.7
c (Å)	31.3	31.5	30.7
β (°)	112.2	109.9	111.2
z	2	2	2
Solvent content (ϕ_s)	16.9	17.6	9.4
Observations	7,408	13,358	5,932
Unique reflections	4,569	4,847	3,175
Maximum resolution Å	2.1	2.1	2.3
Data completeness (%)	86	90	86
Reflections with $I > 2\sigma(I)$ in the range 10–resolution$_{max}$ Å	4,417	4,237	2,705
R_{merge} (%)	3.4	6.3	4.1
R factor	0.186	0.193	0.196
R_{free}	0.265	0.283	0.304
Number of protein atoms	1001	997	992
Number of water oxygens	105	78	46
Estimated coordinate error	0.13	0.15	0.20
RMS deviations (Å) in			
Bond distance	0.011	0.012	0.012
Angle distance	0.040	0.044	0.047

[a] $R_{merge} = \frac{\Sigma\Sigma|I_i - \langle I\rangle|}{\Sigma\Sigma I_i}$; R-factor $= \frac{\Sigma|F_o - F_c|}{\Sigma F_o}$, where I_i is the intensity in the ith measurement of a given reflection, $\langle I\rangle$ the average value, and F_o and F_c are the observed and calculated structure factors.

Intensity data for W17I, W17II, and W9 were collected using a Siemen's Nicolet Area Detector mounted on a Marconi Avionics rotating anode X-ray source. The data were processed using the XENGEN suite of programs.[40,41] Relevant statistics pertaining to the data are given in Table I.

Structure Solution and Refinement

The unit cell dimensions of the three very-low-solvent-content forms are substantially different from those of the two normally hydrated forms (W32 and W22), whose structures are known. Molecular replacement (MR) solutions of W17I and W9 could be obtained uneventfully using MERLOT[42] with the molecule in W22 as the search model. However, the similarly obtained MERLOT solution for W17II

would not refine. Eventually the X-PLOR[43,44] solution using W17I as the search model did.

All three structures were refined in nearly the same manner. The coordinates obtained using the MR solutions were directly used for refinement using PROLSQ[45,46] available in the CCP4 package.[47] Typically, after every 10 to 15 cycles of refinement, $F_o - F_c$ and $2F_o - F_c$ maps were computed and carefully examined. The model was corrected and rebuilt wherever necessary using FRODO.[48] At each stage, the tendency was toward the side of caution to ensure that the model did not contain incorrectly placed atoms. Particular attention was paid to atoms associated with high B values and low density. Usually, positional and thermal parameters were refined in alternate cycles. Refinement using PROLSQ was followed by simulated annealing using X-PLOR.[49–51] The resulting model was carefully checked against electron density maps as well as the input model. Particular attention was paid to those regions of the molecule where initial and final models differed markedly. The model was thoroughly checked at this stage using PROCHECK[52] and necessary corrections were introduced in it. Attention was also paid to the atomic numbering scheme to ensure that the IUPAC-IUB nomenclature[53] is followed.

The refinement was continued using PROLSQ. Once it converged, typically around an R value of 0.22, identification of water molecules began. This was done in several stages with the help of $2F_o - F_c$ and $F_o - F_c$ maps. Cycles of PROLSQ refinement, corrections of model using Fourier maps, and the identification of water molecules continued until no significant density was left in the maps.

At this stage, a one-eighth removed omit map[54–56] was computed. Such a map is formally independent of the input coordinates and provides an unbiased representation of the structure. The model was thoroughly checked against this map and the necessary corrections were introduced. The model was further checked using PROCHECK for its geometrical acceptability. A few more cycles of PROLSQ refinement, accompanied by examination of $F_o - F_c$ and $2F_o - F_c$ maps, were carried out to further correct the model and to identify additional water molecules. Refinement converged with R values in the range of 0.196 to 0.186. Table I contains the summary of refinement statistics. The Ramachandran plots, prepared using PROCHECK, exhibit distributions appropriate for the resolutions of the three structures. Hydrogen bonds in the structure were delineated using the criteria employed in the earlier studies involving water-mediated transformations.[18,21,22]

In view of the unusual nature of the crystals and the importance of the results drawn from their analysis, it appeared desirable to ensure that the refined models were indeed reliable, although the refinement was carried out with great care. Therefore, the final models were further refined with X-PLOR (1) using all reflections in each data set; (2) employing group displacement parameters, one for all mainchain atoms of each residue and another for all sidechain atoms of the residue; and (3) using both (1) and (2). Thus, three more refined models were generated for each structure in addition to the original one obtained largely through refinement using PROLSQ. The root mean square (RMS) deviations in atomic coordinates, including those of water molecules, between any pair of models for the same structure was in no case greater than 0.22 Å.

The coordinates and structure factors have been deposited in the Protein Data Bank. The entry numbers for the coordinates of W17I, W17II, and W9 are 1XEI, 1XEJ, and 1XEK, respectively, while those for the structure factors are R1XEISF, R1XEJSF, and R1XEKSF.

RESULTS AND DISCUSSION

As illustrated in Figure 1, the lysozyme molecule is considered to consist of two domains; domain I is made up of an N-terminal segment (residues 1–38) and a C-terminal segment (residues 88–129), while domain II is a contiguous stretch of polypeptide chain (residues 39–87).[57] The secondary-structural features in the molecule are: α-helices 5–15 (H1), 25–36 (H2), 88–101 (H3), 109–115 (H4); $\alpha/3_{10}$ helices 80–84 (H5), 120–124 (H6); β-sheets 42–63 (S1), 1–3, 38–40 (S2); loops 16–24 (L1), 65–73 (L2), 74–79 (L3), 85–87 (L4), 102–108 (L5), 116–119 (L6); and the C-terminal residues 125–129 (CT).

Variation in Molecular Structure

The RMS deviations in α-carbon positions between different structures obtained after pairwise superposition of protein molecules using InsightII are listed in Table II. Also listed are numbers of mainchain atoms that deviate by more than 1.0 Å. Clearly the changes in the overall structure from that in the native form progressively increase as the level of hydration is systematically reduced. However, on the average, the differences between W32A and W32B on the one hand and W22 on the other are similar in magnitude to those between W32A and W32B. Indeed, the changes resulting from the reduction of the solvent content from 32% to 22% are comparatively small, though significant, and, as we have shown earlier, are similar to those that occur during enzyme action.[32] Further removal of water from the environment of the protein appears to lead to larger changes in atomic positions. It is also interesting that W22 diffracts better than W32, but the diffraction pattern progressively deteriorates with further reduction in solvent content. Indeed, W22 is the best-defined structure in the series and it probably provides the most accurate description of the active molecule. Therefore, in much of what

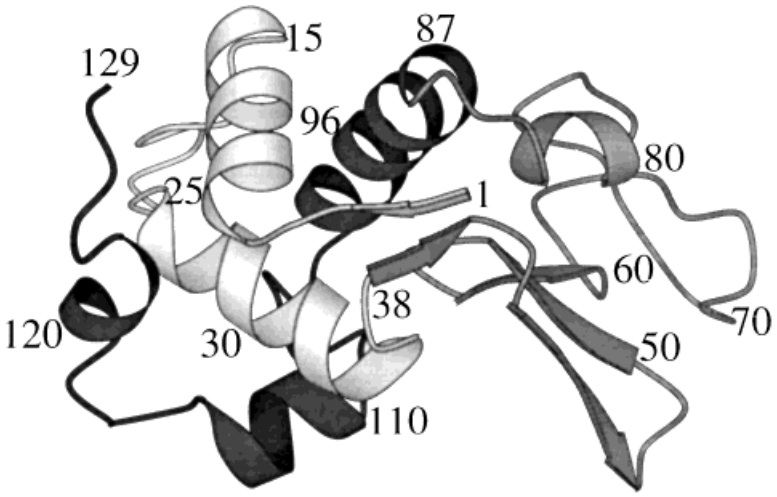

Fig. 1. The lysozyme molecule. The N-terminal segment (residues 1-38) of domain I, the C-terminal segment (residues 88–129) of domain I and domain II (residues 39–87) are in light grey, dark and grey respectively. Figure generated using MOLSCRIPT.[64]

TABLE II. RMS Deviations (Å) in α-Carbon Positions, Where the Number of Mainchain Atoms That Deviate by 1 Å or More in Each Pair is Also Indicated

	W32B	W22	W17I	W17II	W9
W32A	0.46	0.43	0.72	0.79	0.93
	17	15	76	74	158
W32B		0.53	0.68	0.79	0.98
		26	59	76	160
W22			0.64	0.79	0.89
			57	74	134
W17I				0.60	0.92
				50	136
W17II					0.96
					139

TABLE III. RMS Deviations (Å) in α-Carbon Positions From Those in W22, Where Only Those Structural Elements in Which At Least One Value Is Greater Than 0.4 Å Is Included

Structural element	W17I	W17II	W9
Domian I [(1–38) + (88–129)]	0.58	0.72	0.88
N-terminal segment of domian I (1–38)	0.31	0.43	0.57
C-terminal segment of domian I (88–129)	0.69	0.87	1.03
Domian II (39–87)	0.61	0.73	0.81
Helix 3 (88–101)	0.31	0.27	0.52
Helix 4 (109–115)	0.20	0.25	0.45
Helix 6 (120–124)	0.24	0.15	0.59
Sheet 1 (42–63)	0.45	0.54	0.62
Loop 1 (16–24)	0.20	0.25	0.62
Loop 2 (65–73)	0.57	0.62	0.72
Loop 5 (102–108)	0.31	0.30	0.85
Loop 6 (116–119)	0.18	0.23	0.98
C-terminal loop (125–129)	1.01	1.61	1.27

follows, the very-low-solvent-content forms would be described in relation to W22.

Detailed calculations show that variation in solvent content does not lead to substantial changes in the hinge angle involving the centroids of the two domains and the hinge region, as defined by McCammon et al.[58] Systematic variations in the mutual juxtaposition of different pairs of secondary-structural elements as a function of the level of hydration could not also be detected. However, the atomic deviations within different segments of the molecule and different secondary-structural elements exhibit considerable variation. RMS deviations in α-carbon positions in different structural elements from those in W22 in cases where at least one value exceed 0.4 Å are listed in Table III.

The RMS deviations in the two domains are nearly at the same level. However, the C-terminal segment of domain I is clearly much more flexible than the N-terminal segment. Considerable variation in flexibility exists among different secondary-structural elements as well. Admittedly, other things being equal, the RMS deviation on superposition tends to increase when the length of the peptide chain increases, and the lengths of the different secondary-structural elements are not the same. Yet, the observed RMS deviations provide a rough and ready estimate of the flexibility. The only flexible secondary-structural element in the N-terminal segment of domain I is the 16–24 loop. The loop does not undergo large changes in the internal structure when the solvent content is reduced to 17%; the changes become substantial when the solvent content is reduced still further to 9%. A similar situation exists with respect to three helices (88–101, 109–115, and 120–124) and two loops (102–108 and 116–119) in the C-terminal segment of domain I, while large deviations are exhibited by the C-terminal residues (125–129) in all the three structures. The main β-sheet in the structure (residues 42–63) dominates domain II. The RMS deviations are substantial in the sheet partly because of the

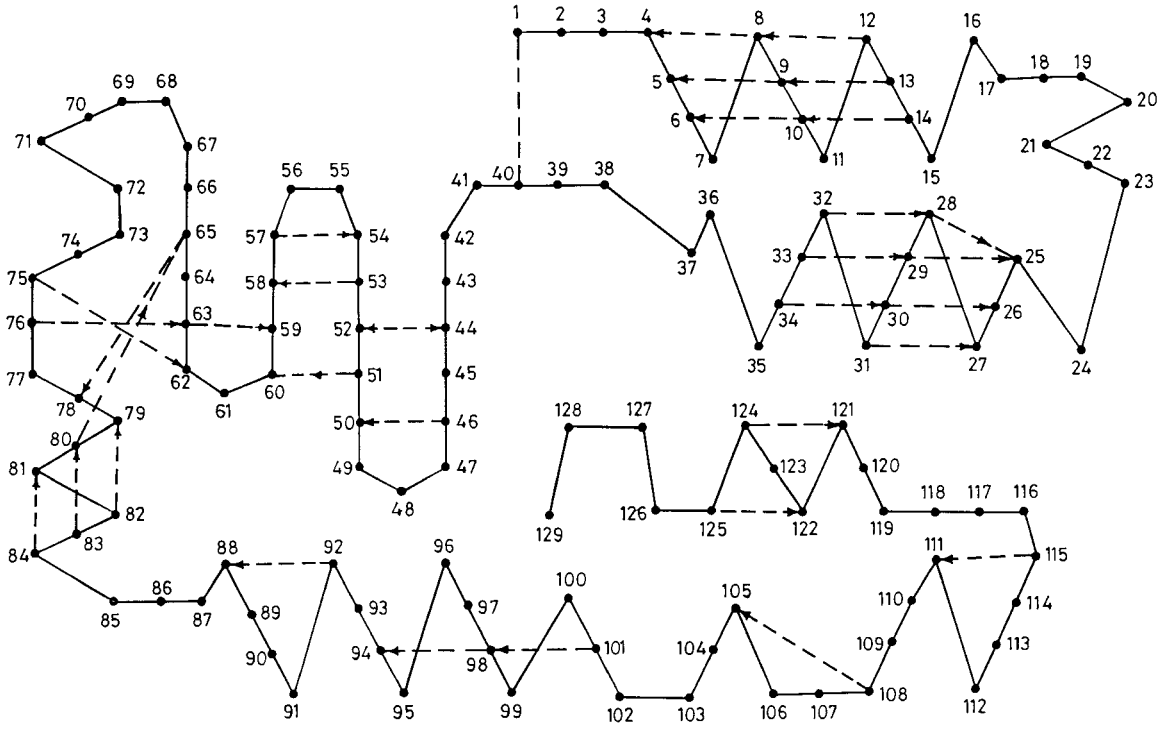

Fig. 2. Main chain-main chain hydrogen bonds present in all the structures.

length of the polypeptide chain constituting it. The structural feature that is highly flexible in this domain is undoubtedly the 65–73 loop.

At least one mainchain conformational angle (ϕ or ψ)[59] differs by 60° or more from that in W22 in one or the other of the very-low-humidity structures in the case of 31 residues. Of these eight are glycines, which are known to be flexible. Three are alanines, while small hydrophilic residues such as threonine, serine, aspartic acid, and asparagine account for nine residues. Thus, flexibility caused by changes in hydration appears to involve primarily glycine and residues with small, mostly hydrophilic, sidechains. Interestingly, 18 of the 31 residues are among the 42 residues that constitute the C-terminal segment of domain I. The N-terminal segment consisting of 33 residues account for five and domain II (46 residues) for the remaining eight. Not surprisingly, all except three of the 31 residues belong to what have been shown earlier to belong to the moderately flexible regions of the molecule.[19] There are 16 residues, which form a subgroup of the 31, in which two or more of the six mainchain conformational angles in the three very-low-humidity forms change by 60° or more from those in W22. Of these, 12 occur in three stretches (67–72, 101–103, and 127–129) involving three or more contiguous residues. These stretches largely form part of the 65–73 and 102–108 loops and the C-terminus.

The number of mainchain–mainchain hydrogen bonds in the six crystallographically independent molecules in the five structures (the three reported here and the normally hydrated forms W32 and W22) is similar and varies between 70 and 80. However, only 35 of these, shown in Figure 2, occur in all the structures. Of these, only six are present in the C-terminal segment of domain I, although the segment accounts for nearly a third of the molecule. Changes in hydrogen bonding pattern is obviously an index of conformational changes and the paucity of conserved hydrogen bonds in this segment reiterates its flexibility. The decrease in conserved hydrogen bonds in the secondary-structural regions also broadly conform to the increased flexibility as evidenced by RMS deviations in α-carbon positions.

To sum up, reduction in the level of hydration causes considerable deviation in atomic positions. Understandably, the deviations from the positions in the native structure is the highest in the structure with the lowest level of hydration. The deviations are not, however, uniformly distributed in the molecule. Nor are they related to changes in intermolecular contacts from the variation in the solvent content. They are the highest in the C-terminal segment of domain I and the main loop in domain II, indicating the higher flexibility of these regions of the molecule. A comparison of the mainchain torsion angles and the mainchain–mainchain hydrogen bonds in different structures corroborates this conclusion. It highlights the extreme flexibility of the loops 65–73 and 102–108 and the five C-terminal residues.

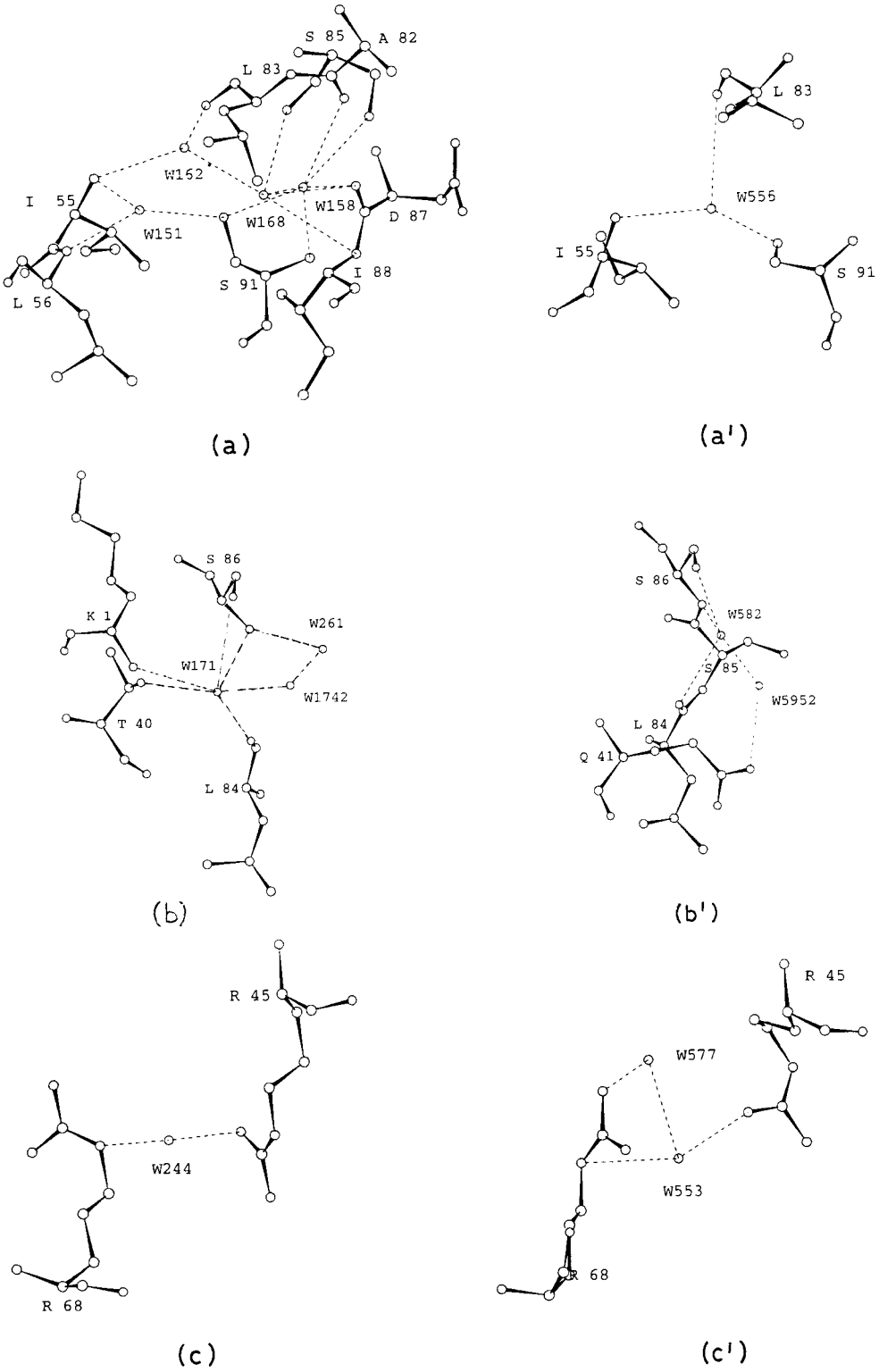

Fig. 3. Water bridges involved in long range interactions with elements of commonality between W22 (unprimed) and W9 (primed). This figure and the subsequent ones were generated by InsightII©. Please see text for details.

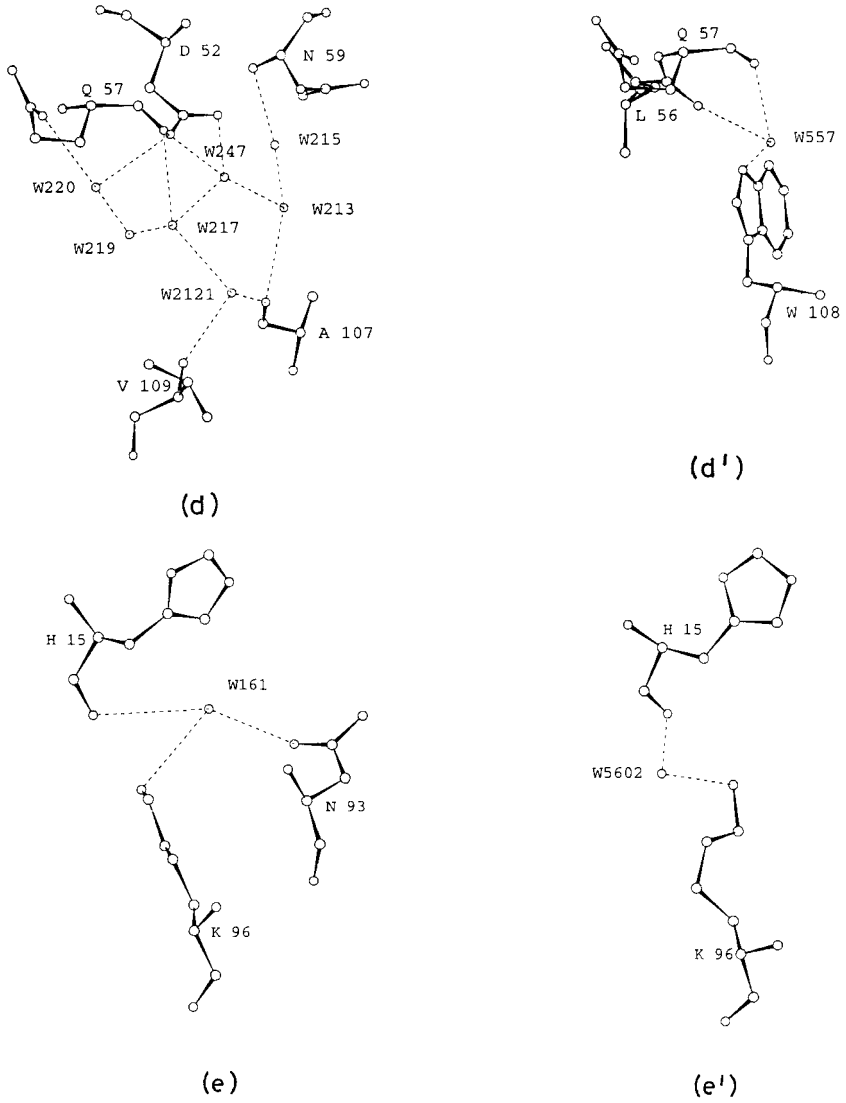

Figure 3. (Continued.)

Hydration Shell and Water-Mediated Tertiary Interactions

Water molecules that are at a distance of 3.6 Å or less from the nitrogen or oxygen atoms of the protein molecule is considered to constitute its hydration shell.[18,21,22,32] The numbers of such water molecules in W32A, W32B, W22, W17I, W17II, and W9 are 125, 131, 173, 129, 89, and 60, respectively. The number of molecules in the hydration shell depends not only on the water content, but also on the number that could be located from the electron density maps. In the five structures considered, W22 is the most ordered and the crystals diffract to a higher resolution than the other forms do. Therefore, the number of water molecules per protein molecule is the highest in W22, which is higher than in the native crystals. The two W17 forms have similar water contents, but the quality of the crystals is better in form I than in form II. Therefore W17I has more located ordered water molecules in its hydration shell than W17II. Of course, W9 contains the least number of water molecules in its shell.

Despite the differences in water content and the number of located water molecules in the hydration shell, the nature of hydration is similar in all the structures. For instance, the number of protein–water interactions involving oxygen atoms are larger than the number of those involving nitrogen atoms. The proportion of hydrated sidechain atoms are more than that of the hydrated mainchain atoms in all the structures. The shell in each case is made up of discon-

tinuous patches on the protein surface. Clusters of two water molecules and three water molecules exist in all the structures. The number of large clusters are very few.

A majority of water molecules in each shell interact with only one protein atom. Those that interact with more than one protein atom give rise to water bridges. Many of these bridges involve atoms of the same residue or atoms separated by five residues or less. Such local bridges often give rise to favorable sites of hydration.[18,21,22] As in other structures, sidechains with multiple hydrogen bonding centers, and regions between short hydrophilic sidechains and the CO or NH group of the same or a nearby residue, often constitute such sites in the very-low-humidity forms.

The local bridges presumably also stabilize local conformation. More important perhaps are water bridges involving atoms widely separated along the polypeptide chain. Such bridges, which exist in all the forms, are involved in holding different regions of the molecule together. It is of particular interest to inquire as to what extent such bridges remain invariant with respect to changes in the level of hydration. Water bridges in all five structures were carefully examined with this objective in view. Attention was concentrated on W22 and W9, the two forms with the largest and the least number of water molecules in their hydration shells. Admittedly, water positions in W9 are less precisely defined on account of lower resolution of the data. However, the emphasis in the present analysis is not on the precise location of water molecules, but on their presence in specific regions.

The different sets of long-range water bridges with elements of commonality between W22 and W9 are illustrated in Figure 3. Four water molecules are involved in W22 in connecting the 80–84 helix, the 88–101 helix, and the main β-sheet (Fig. 3a). The number of water molecules in this region decreases in W9, and a single water molecule connects residues 83 and 91 with residue 55 in the main β-sheet (Fig. 3a′). In the second set (Fig. 3b and b′), water bridges connect the junction between the major and the minor β-sheets with the region between 80–84 and 88–101 helices. The third set (Fig. 3c and c′) is concerned with interaction between the main β-sheet and the main loop. The connection of the main β-sheet with the loop connecting helices 88–101 and 109–115 is made up of several bridges involving seven water molecules in W22 (Fig. 3d). Many of these water molecules are absent in W9. Yet the connectivity is maintained through water bridges involving a single water molecule. There are differences even in the protein atoms involved, yet the basic function of connecting the two regions is fulfilled. Helices 5–15 and 88–101, belonging to the two segments of domain I, are interconnected through water bridges in both the structures (Fig. 3e and e′).

The comparison between the water bridges in W22 and W9 clearly indicate that many crucial water-mediated connectivities between different regions of the molecule, which are obviously important for the structural integrity of the protein, are essentially conserved inspite of differences in detail. These connectivities, with differences in detail, exist in monoclinic lysozyme at various levels of hydration and in the other crystal forms of lysozyme also. The results clearly demonstrate that water-mediated tertiary interactions important for the integrity of the protein structure are retained even when the crystal is dehydrated with concentrated sulfuric acid below the level needed for activity, as in W9. The very low water content of 9.4% in W9 perhaps also sets the limit beyond which water molecules cannot be removed from the protein molecule without destroying the tertiary structure.

Hydration and Geometry of Active Site

As indicated earlier, among the crystal forms considered, W22 is likely to be the form with the lowest solvent content having fully active protein molecules. The molecules in W17I and W17II could represent a marginal case in terms of activity. W9, with a solvent as low as 9.4%, is likely to be made of inactive molecules. Yet the molecules in all these forms, as indeed those in W32, have essentially the same tertiary structure. Thus it would appear that the loss of activity consequent to the reduction of the level of hydration below 0.2-g water/g protein[4,8] is not caused by any drastic change in the three-dimensional structure; the cause perhaps lies in the hydration and the geometry of the active-site region.

The active-site cleft is a heavily hydrated region of the lysozyme molecule. Furthermore, several water molecules forming part of a network spanning the cleft remain invariant in the five well-refined, normally hydrated crystal structures of the enzyme.[19,21] This network in W22 is illustrated in Figure 4a. The number of water molecules is much lower in the very-low-solvent-content forms. This feature is particularly striking in W9 (Fig. 4b), in which, for instance, there is only one water molecule involved in a bridge across the cleft. Presumably, the water molecules in the cleft are important for enzyme action, admittedly in some as yet unknown way, especially as several of them remain invariant in the normally hydrated forms.[19] The removal of many of these might be a highly probable cause for the loss of activity at very low levels of hydration.

Another interesting observation pertaining to activity concerns the size of the binding cleft. The size decreases with decreasing level of hydration. This is immediately obvious from the profiles of solvent-accessible surface area shown for W22 and W9 in Figure 5. The conclusion was reinforced by calculations using program VOIDOO.[60] Calculations were

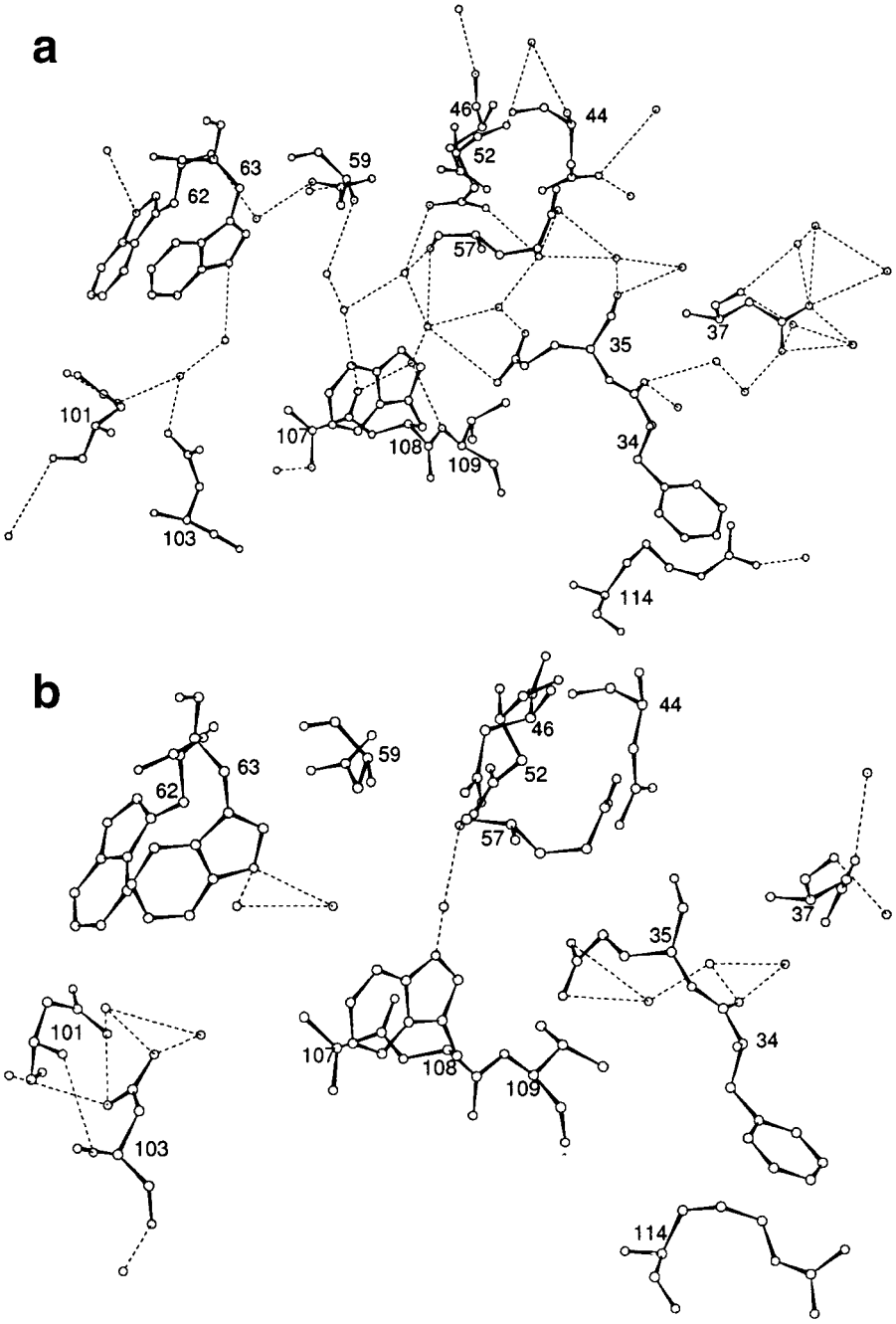

Fig. 4. Hydration and water network in the active site of (**a**) W22 and (**b**) W9.

performed using a region of the molecule made up of all the residues within 6 Å from any of the inhibitor/substrate atoms in the crystal structures of well-refined enzyme-inhibitor complexes and the modeled sugar of the hexasaccharide substrate complex.[61–63] In order to eliminate random errors, each calculation was repeated 10 times, with exactly the same input parameters (probe radius = 1.4 Å, grid spacing = 1.0 Å, atomic fattening factor = 1.1 Å, grid-shrink factor = 0.9 Å, number of volume calculation cycles = 10), but with randomly rotated copies of the region. They yielded average accessible volumes of 115.6, 114.0, 97.1, 83.6, 81.2, and 37.1 $Å^3$ for W32A, W32B, W22, W17I, W17II, and W9, respectively. The superposition of the binding site residues in W22 and W9 (Fig. 6) illustrates the reduction in width of the cleft, as do the closest approaches, given in Table IV, between residues facing one-another across the cleft indicate. The role of Trp62 and Trp63 in reducing the width of the cleft is particularly noteworthy.

Thus, to sum up, the loss of activity accompanying dehydration appears to be caused by the removal of

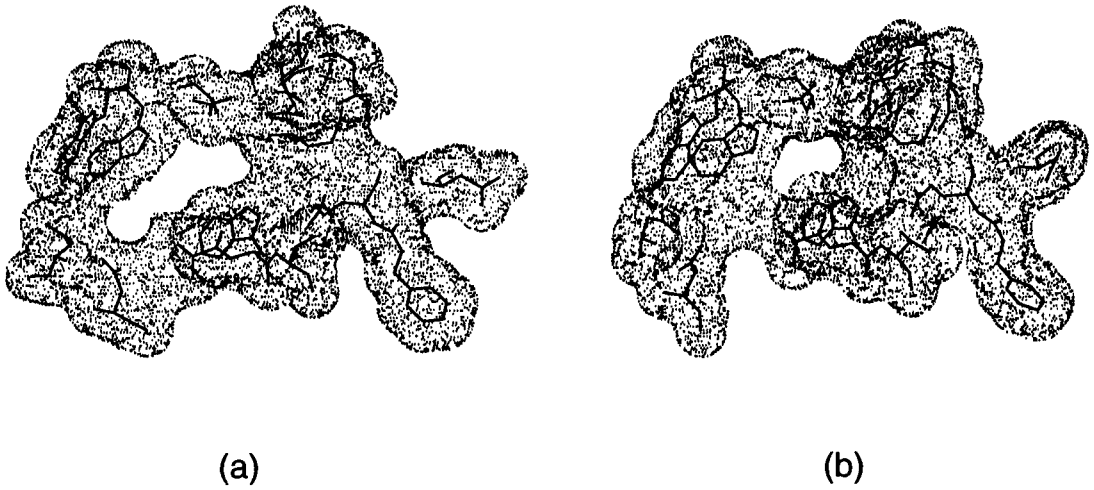

Fig. 5. Solvent Accessible surface area profiles of the active site region in (**a**) W22 and (**b**) W9.

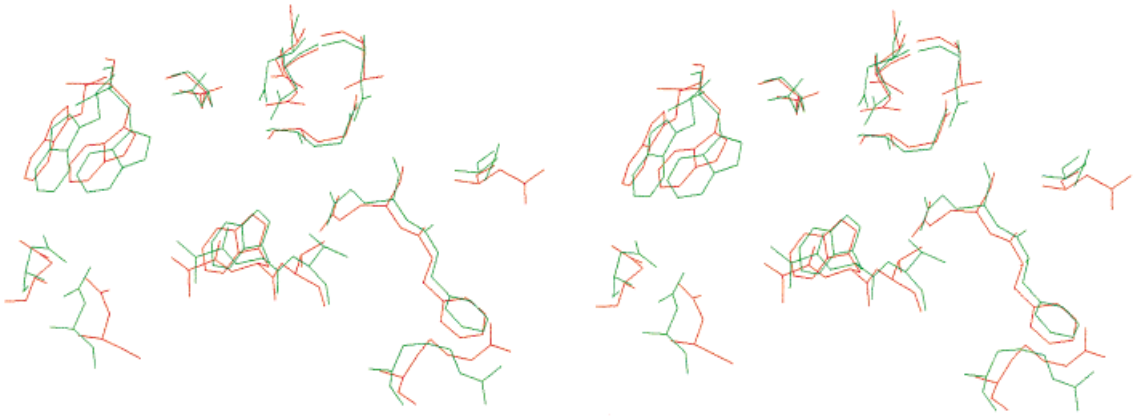

Fig. 6. Stereoview of the superposition of active site residues in W22 (red) and W9 (green).

TABLE IV. Closest Approaches of Residues That Lie on the Opposite Sides of the Active-Site Cleft in W22 and W9

	Distance (Å)	
	W22	W9
Asn37–Phe34	4.7	4.4
Asn37–Glu35	3.8	4.0
Asp52–Glu35	6.1	5.1
Gln57–Glu35	3.4	3.1
Asp52–Ala107	7.8	6.3
Asp52–Trp108	8.0	6.3
Asp52–Val109	7.6	7.6
Gln57–Ala107	6.6	6.6
Gln57–Trp108	4.9	4.4
Gln57–Val109	7.4	7.6
Trp62–Asp101	4.7	4.1
Trp62–Asn103	6.4	4.6
Trp63–Asp101	4.5	3.3
Trp63–Asn103	5.6	4.8

functionally important water molecules from the active-site region and the reduction in the size and width of the cleft.

CONCLUSIONS

The present study, in which a lysozyme crystal could be examined at extremely and unprecedentedly low levels of hydration, demonstrates that the enzyme can retain its three-dimensional structure even when the water associated with it is much lower than that required for activity. Interestingly, the long-range water-mediated interactions that contribute to the stability of the tertiary structure are essentially retained even at a very low solvent content of 9.4%, which perhaps sets the critical limit below which the three-dimensional structure of the enzyme might collapse.

Changing the amount of water associated with protein molecules and following the resultant alterations in

the molecular structure is the gentlest way of investigating the inherent flexibility or deformability of the different regions of the protein molecule. In the present investigations, the lysozyme molecule has been examined at widely different levels of hydration and the results have provided definite information on the deformability of different segments of the enzyme molecule.

A comparison of the very-low-solvent-content forms with the normally hydrated forms provides valuable insights into the role of water in the action of lysozyme. In particular, it provides a plausible explanation as to how the molecule loses its activity even when the three-dimensional structure remains substantially intact. It highlights the importance of water network in the active-site cleft for the activity of the enzyme. The structure of the 9.4% water content form also demonstrates that the active-site cleft shrinks and causes the enzyme to be inactive when it is excessively dehydrated.

ACKNOWLEDGMENTS

The diffraction data were collected on the Area Detector/Image Plate Facility funded by the Department of Science and Technology (DST) and the Department of Biotechnology (DBT). The computations and map-fitting were carried out at the Supercomputer Education and Research Centre and the DBT-funded Graphics Facility. We thank Moses M. Prabu for help in preparing figures.

REFERENCES

1. Kuntz, I.D., Jr., Kauzmann, W. Hydration of proteins and polypeptides. Adv. Protein Chem. 28:239–345, 1974.
2. Finney, J.L., Gellaty, B.J., Golton, I.C., Good Fellow, J.M. Solvent effects and polar interactions in the structural stability and dynamics of globular proteins. Biophys. J. 32:17–33, 1980.
3. Tanford, C. "The Hydrophobic Effect: Formation of Micelles and Biological Membranes," 2nd edit. New York: John Wiley & Sons, Inc., 1980.
4. Rupley, J.A., Gratton, E., Careri, G. Water and globular proteins. Trends Bio. Sci. 8:18–22, 1983.
5. Saenger, W. Structure and dynamics of water surrounding biomolecules. Ann. Rev. Biophys Chem. 16:93–114, 1987.
6. Sundaralingam, M., Shekarudu, Y.C. Water-inserted alpha-helical segments implicate reverse turns as folding intermediates. Science 244:1333–1337, 1989.
7. Dill, K.A. Dominant forces in protein folding. Biochemistry 29:7133–7155, 1990.
8. Rupley, J.A., Careri, G. Protein hydration and function. Adv. Protein Chem. 41:37–172, 1991.
9. Sharp, K.A. The hydrophobic effect. Curr. Opin. Struct. Biol. 1:171–174, 1991.
10. Teeter, M.M. Water–protein interactions: Theory and experiment. Annu. Rev. Biophysics. Chem. 20:577–600, 1991.
11. Westhof, E. "Water and Biological Macromolecules." Boca Raton: CRC Press, 1994.
12. Karplus, P.A., Faerman, C. Ordered water in macromolecular structure. Curr. Opin. Struc. Biol. 4:770–776, 1994.
13. Poornima, C.S., Dean, P.M. Hydration in drug design. I. Multiple hydrogen-bonding features of water molecules in mediating protein–ligand interactions. J. Comp.-aided Mol. Design 6:500–512, 1985.
14. Blake, C.C.F., Pulford, W.C.A., Artymiuk, P.J. X-ray studies of water in crystals of lysozyme. J. Mol. Biol. 167:693–723, 1983.
15. Teeter, M.M. Water structure of a hydrophobic protein at atomic resolution: Pentagon rings of water molecules in crystals of crambin. Proc. Natl. Acad. Sci. U.S.A. 81:6014–6018, 1984.
16. Savage, H., Wlodawer, A. Determination of water structure around biomolecules using X-ray and neutron diffraction methods. Methods Enzymol. 127:162–183, 1986.
17. Baker, E.N., Blundell, T.L., Cutfield, J.F., et al. The structure of 2Zn pig insulin crystals at 1.5 Å resolution. Phil. Trans. Roy. Soc. London 319:369–456, 1988.
18. Kodandapani, R., Suresh, C.G., Vijayan, M. Crystal structure of low humidity tetragonal lysozyme at 2.1-Å resolution. J. Biol. Chem. 265:16126–16131, 1990.
19. Madhusudan, Vijayan, M. Rigid and flexible regions in lysozyme and the invariant features in its hydration shell. Curr. Sci. 60:165–170, 1991.
20. Malin, R., Zielenkiewicz, P., Saenger, W. Structurally conserved water molecules in ribonuclease T1. J. Biol. Chem. 266:4848–4852, 1993.
21. Madhusudan, Kodandapani, R., Vijayan, M. Protein hydration and water structure: X-ray analysis of a closely packed protein crystal with very low solvent content. Acta Cryst. D49:234–245, 1993.
22. Radha Kishan, K.V., Chandra, N.R., Sudarsanakumar, C., Suguna, K., Vijayan, M. Water-dependent domain motion and flexibility in ribonuclease A and the invariant features in its hydration shell: An X-ray study of two low-humidity-crystal forms of the enzyme. Acta Cryst. D51:703–710, 1995.
23. Schoenborn, B.P., Garcia, A., Knott, R. Hydration in protein crystallography. Progs. Biophys. Mol. Biol. 64:105–119, 1995.
24. Kennedy, S.D., Bryant, R.G. Structural effects of hydration: Studies of lysozyme by ^{13}C solids NMR. Biopolymers 29:1801–1806, 1990.
25. Otting, G., Liepinsh, E., Wuthrich, K. Protein hydration in solution. Science 254:974–980, 1991.
26. Belton, P.S. NMR studies of protein hydration. Prog. Biophys. Mol. Biol. 61:61–79, 1994.
27. Arytymiuk, P.J., Blake, C.C.F., Grace, D.E.P., Oatley, S.J., Phillips, D.C., Sternberg, M.J.E. Crystallographic studies of the dynamic properties of lysozyme. Nature 280:563–568, 1979.
28. Vijayan, M., Salunke, D.M. Structural mobility and transformations in globular proteins. J. Bio. Sci. 6:357–377, 1984.
29. Ringe, D., Petsko, G.A. Mapping protein dynamics by X-ray diffraction. Progs. Biophys. Mol. Biol. 45:197–235, 1985.
30. Caspar, D.L.D., Badger, J. Plasticity of crystalline proteins. Curr. Opi. Struc. Biol. 1:877–882, 1991.
31. Morozov, V.N., Morozova, T.Y. Elasticity of globular proteins: The relation between mechanics, thermodynamics and mobility. J. Biomol. Struct. Dyn. 11:459–481, 1993.
32. Nagendra, H.G., Sudarsanakumar, C., Vijayan, M. An X-ray analysis of native monoclinic lysozyme: A case study on the reliability of refined protein structures and a comparison with the low-humidity form in relation to mobility and enzyme action. Acta Cryst. D52:1067–1074, 1996.
33. Salunke, D.M., Veerapandian, B., Vijayan, M. Water-mediated structural transformations in a new crystal form of ribonuclease A and tetragonal lysozyme. Curr. Sci. 53:231–235, 1984.
34. Salunke, D.M., Veerapandian, B., Kodandapani, R., Vijayan, M. Water-mediated transformations in protein crystals. Acta Cryst. B41:431–436, 1985.
35. Nagendra, H.G., Sudarsanakumar, C., Vijayan, M. Characterization of lysozyme crystals with unusually low solvent content. Acta Cryst. D51:390–392, 1995.
36. Matthews, B.W. Solvent content of protein crystals. J. Mol. Biol. 33:491–497, 1968.
37. Steinrauf, L.K. Preliminary X-ray data for some new crystalline forms of β-lactoglobulin and hen-egg-white lysozyme. Acta Cryst. 12:77–79, 1959.
38. Rockland, L.B. Saturated salt solutions for static control of relative humidity between 5° and 40°C. Anal. Chem. 32:1375–1376, 1960.

39. Weast, R.C., Astle, M.J. (eds.). "CRC Handbook of Chemistry and Physics." Boca Raton: CRC Press, 1980:E46.
40. Howard, A.J., Gilliland, G.L., Finzel, B.C., Poulos, T.L., Ohlendorf, D.H., Salemme, F.R. The use of an imaging proportional counter in macromolecular crystallography. J. Appl. Cryst. 20:383–387, 1987.
41. XENGEN manual. Madison: Nicolet Instrument Corporation, 1987.
42. Fitzgerald, P.M.D. MERLOT, an integrated package of computer programs for the determination of crystal structures by molecular replacement. J. Appl. Cryst. 21:273–278, 1988.
43. Huber, R. Experience with the application of Patterson search techniques. In "Molecular Replacement." Proceedings of the Daresbury study weekend, SERC Daresbury laboratory, Warrington, England, 1985:58–61.
44. Brunger, A.T. Extension of molecular replacement: A new search strategy based on Patterson correlation refinement. Acta Cryst. A46:46–57, 1990.
45. Hendrickson, W.A., Konnert, J.H. Incorporation of stereochemical information into crystallographic refinement. In: "Computing in Crystallography." Diamond, R., Ramaseshan, S., Venkatesan, K. (eds.). Bangalore: Indian Academy of Sciences, 1980:13.01–13.26.
46. Hendrickson, W.A. Stereochemically restrained refinement of protein structures. Methods Enzymol. 115:252–270, 1985.
47. Computational Collaborative Project, Number 4. Acta Cryst. D50:760–763, 1994.
48. Jones, T.A. A graphics model building and refinement system for macromolecules. J. Appl. Cryst. 11:268–272, 1978.
49. Brunger, A.T., John, K., Karplus, M. Crystallographic R factor refinement by molecular dynamics. Science 235:458–460, 1987.
50. Brunger, A.T., Krukowski, A. Slow-cooling protocols for crystallographic refinement by simulated annealing. Acta Cryst. A46:585–593, 1990.
51. Brunger, A.T. Simulated annealing in crystallography. Annu. Rev. Phys. Chem. 42:197–223, 1991.
52. Laskowski, R.A., MacArthur, M.W., Moss, D.S., Thornton, J.M. PROCHECK: A program to check the stereochemical quality of protein structures. J. Appl. Cryst. 26:283–291, 1993.
53. IUPAC-IUB Commision on Biochemical Nomenclature. J. Mol. Biol. 52:1–17, 1970.
54. Vijayan, M. On the Fourier refinemet of protein structures. Acta Cryst. A36:295–298, 1980.
55. Dodson, G.G. In: "Refinement of Protein Structures. Proceedings of the Daresbury Weekend." Machin, P.A., Campbell, J.W., Elder, M. (eds.). Daresbury: SERC, 1981:95–98.
56. Bhat, T.N., Cohen, G.H. OMITMAP: An electron density map suitable for the examination of errors in a macromolecular model. J. Appl. Cryst. 17:244–248, 1984.
57. Janin, J., Wodak, S.J. Structural domains in proteins and their role in the dynamics of protein function. Prog. Biophys. Molec. Biol. 42:21–78, 1983.
58. McCammon, J.A., Gelin, B.R., Karplus, M., Wolynes, P.G. The hinge-bending mode in lysozyme. Nature 262:325–326, 1976.
59. Ramachandran, G.N., Sasisekaran, V. Conformation of polypeptides and proteins. Adv. Protein Chem. 3:284–438, 1968.
60. Kleywegt, G.J., Jones, A. Detection, delineation, measurement and display of cavities in macromolecular structures. Acta Cryst. D50:178–185, 1994.
61. Cheetam, J.C., Artymuik, P.J., Phillips, D.C. Refinement of an enzyme complex with inhibitor bound at partial occupancy: Hen egg-white lysozyme and tri-N-acetylchitotriose at 1.75-Å resolution. J. Mol. Biol. 224:613–628, 1992.
62. Maenaka, K., Matsushima, M., Song, H., Sunada, F., Watanabe, K., Kumagai, I. Dissection of protein–carbohydrate interactions in mutant hen egg-white lysozyme complexes and their hydrolytic activity. J. Mol. Biol. 247:281–293, 1995.
63. Bernstein, F.C., Koetzle, J.F., Williams, G.J.B., et al. The protein data bank: A computer-based archival file for macromolecular structures. J. Mol. Biol. 112:535–542, 1977.
64. Kraulis, P. MOLSCRIPT: A program to produce both detailed and schematic plots of protein structures. J. Appl. Cryst. 24:946–950, 1991.